nature biotechnology

High-throughput mapping of the chromatin structure of human promoters

Fatih Ozsolak[1,4], Jun S Song[2–4], X Shirley Liu[2,3] & David E Fisher[1]

Our understanding of how chromatin structure influences cellular processes such as transcription and replication has been limited by a lack of nucleosome-positioning data in human cells. We describe a high-resolution microarray approach combined with an analysis algorithm to examine nucleosome positioning in 3,692 promoters within seven human cell lines. Unlike unexpressed genes without transcription-preinitiation complexes at their promoters, expressed genes or genes containing preinitiation complexes exhibit characteristic nucleosome-free regions at their transcription start sites. The combination of these nucleosome data with chromatin immunoprecipitation–chip analyses reveals that the melanocyte master regulator microphthalmia-associated transcription factor (MITF) predominantly binds nucleosome-free regions, supporting the model that nucleosomes limit sequence accessibility. This study presents a global view of human nucleosome positioning and provides a high-throughput tool for analyzing chromatin structure in development and disease.

Transcriptional regulation and many other essential cellular processes, such as replication and DNA repair, are dependent on nucleosome structure and positioning, because nucleosomes limit accessibility to regulatory factors[1,2] and many cellular signaling events affect nucleosome composition and localization[3–5]. The positioning of nucleosomes is probably most critical in promoter and enhancer regions, as it regulates gene expression[6]. Major advances in experimental[7] and computational[8,9] approaches have elucidated nucleosome positioning in yeast. In human cells, however, nucleosome-positioning data are available for only a handful of promoters.

To study nucleosome distribution in human promoters, we performed a genome-wide *in vivo* DNA footprinting experiment on human primary fibroblasts (IMR90), primary melanocytes (PM), mammary epithelial cells (MEC) and melanoma (A375, MALME) and breast cancer cell lines (T47D, MCF7). We isolated mononucleosomal DNA from micrococcal nuclease (MNase) digestions and genomic input DNA from the same cell line (digested to a similar size distribution) as control. Nucleosomal and input DNA were differentially labeled and hybridized to microarrays containing 50-mer probes staggered in 10-base pair (bp) steps and spanning 1.5-kb promoter regions of 3,692 genes, including all genes in the Affymetrix Human Cancer G110 Array.

We devised several signal-processing techniques to analyze the microarray data and identify positioned nucleosomes (**Supplementary Methods** online). Briefly, we used wavelet decomposition followed by outlier averaging to remove high-frequency noise, and subsequently applied Laplacian of Gaussian edge-detection to find peaks and troughs corresponding to positioned nucleosomes and nucleosome-free regions, respectively. The Hidden Markov Model–based algorithm used for yeast nucleosome mapping[7] could not be applied to our microarray data of 1.5-kb promoter fragments, because this algorithm requires contiguously tiled regions. In addition, as repeat sequences are frequently found in the human genome, repeat-masking fragmented many promoters into discontinuous subsegments on our tiling arrays.

We conducted biological replicate experiments on independent mononucleosome isolations from the A375, MALME and IMR90 cell lines. Using a peak-to-trough ratio cutoff that yielded roughly 5% false positives (**Supplementary Discussion** online) and requiring replicate peaks to overlap by at least 80% in sequence, the concordance of both peaks and troughs in the biological replicates within each cell line was ~70% (**Supplementary Discussion**)—a concordance comparable if not better than that of most chromatin immunoprecipitation (ChIP)-chip experiments[10,11]. Most of the remaining 20–30% of peaks was reproducible at lower peak-to-trough ratios; more precisely, as many as 90% of the peaks in one replicate was consistently reproduced in another replicate if we slightly lowered the cutoff threshold. Importantly, preservation of differences in cell line–specific nucleosome positions in the replicates suggests that our analysis method is sufficiently reproducible. Using this approach we observed that promoters of genes with the same expression status in the different cell lines displayed strikingly conserved nucleosome positions, as exemplified by the endothelin-1 promoter (**Fig. 1a**). In addition, positioned nucleosomes occupied 24 ± 3% of an average promoter lengthwise, and 88% of the investigated promoters had at least one positioned nucleosome.

To validate the accuracy of our experimental and analytical methods, we performed a negative-control experiment by hybridizing two

[1]Melanoma Program in Medical Oncology, and Department of Pediatric Oncology, Dana-Farber Cancer Institute, Children's Hospital Boston, Harvard Medical School, 44 Binney Street, Boston, Massachusetts 02115, USA. [2]Department of Biostatistics and Computational Biology, Dana-Farber Cancer Institute, 44 Binney Street, Boston, Massachusetts 02115, USA. [3]Harvard School of Public Health, 677 Huntington Avenue, Boston, Massachusetts 02115, USA. [4]These authors contributed equally to this work. Correspondence should be addressed to D.E.F. (david_fisher@dfci.harvard.edu) or X.S.L. (xsliu@jimmy.harvard.edu).

Received 3 October 2006; accepted 28 November 2006; published online 14 January 2007; doi:10.1038/nbt1279

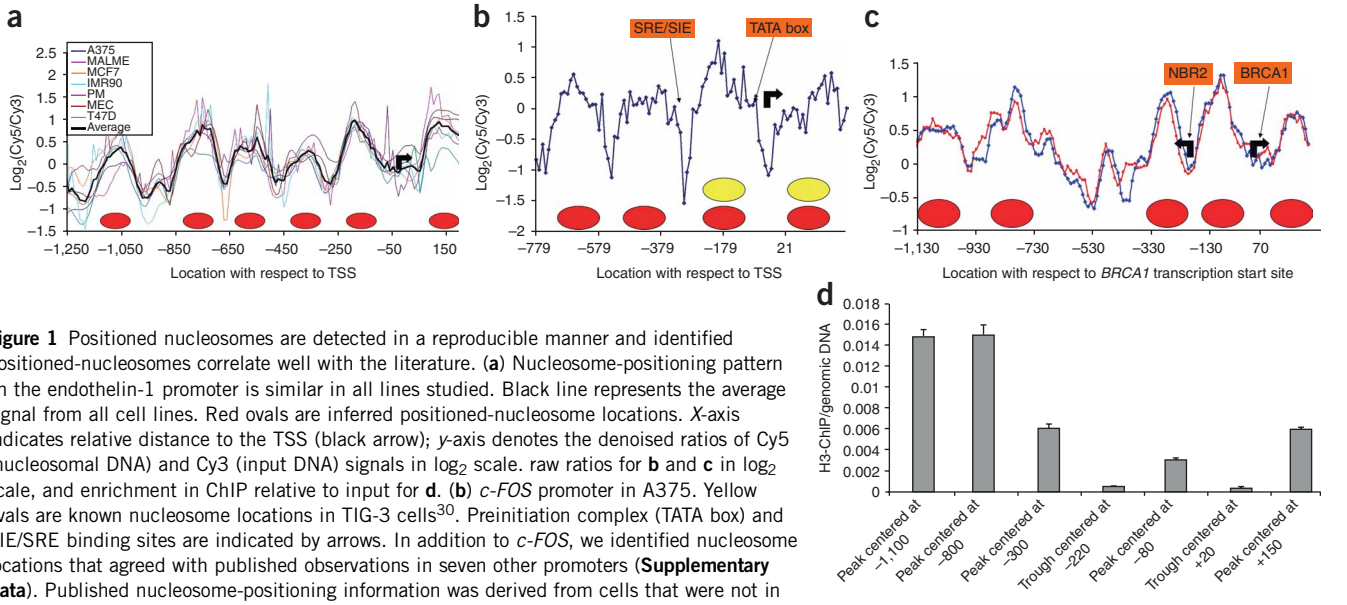

Figure 1 Positioned nucleosomes are detected in a reproducible manner and identified positioned-nucleosomes correlate well with the literature. (**a**) Nucleosome-positioning pattern on the endothelin-1 promoter is similar in all lines studied. Black line represents the average signal from all cell lines. Red ovals are inferred positioned-nucleosome locations. *X*-axis indicates relative distance to the TSS (black arrow); *y*-axis denotes the denoised ratios of Cy5 (nucleosomal DNA) and Cy3 (input DNA) signals in $\log_2$ scale. raw ratios for **b** and **c** in $\log_2$ scale, and enrichment in ChIP relative to input for **d**. (**b**) *c-FOS* promoter in A375. Yellow ovals are known nucleosome locations in TIG-3 cells[30]. Preinitiation complex (TATA box) and SIE/SRE binding sites are indicated by arrows. In addition to *c-FOS*, we identified nucleosome locations that agreed with published observations in seven other promoters (**Supplementary Data**). Published nucleosome-positioning information was derived from cells that were not in our dataset. Nonetheless we observed a high degree of concordance with literature positions and our findings, suggesting that for certain genes nucleosome positioning is highly conserved across different lineages. *Y*-axis shows raw data. (**c**) Reproducibility of nucleosome position determinations at the *BRCA1-NBR2* promoter locus. Red and blue lines represent raw data from the two biological replicates of A375 cells. (**d**) Histone H3 chromatin immunoprecipitations (ChIP) at nucleosome resolution for the A375 *BRCA1-NBR2* promoter. Primers designed for the identified peaks and troughs were used to determine the relative levels of signal amplification in ChIP samples relative to genomic DNA. Primers for the troughs centered at locations –900 and –500 could not be designed because of the local sequence characteristics of the regions. The figure indicates abundant histone H3 protein within the identified peaks relative to troughs.

differentially labeled genomic input DNAs onto our tiling arrays (input/input analysis). Compared to the nucleosome/input samples where neighboring probes demonstrated strong short-range autocorrelation due to coherent DNA fragments that survived the MNase digestion, the input/input sample showed insignificant autocorrelation among neighboring probes. Only a very small number of qualifying peaks was detected in the input/input sample, giving a false-positive rate estimate of 5.5% for our nucleosome/input samples at the fixed parameters used throughout this study (**Supplementary Discussion**).

We isolated mononucleosomes by rapid cell permeabilization and partial digestion of chromatin. It was possible that cross-linking the cells before nucleosome isolation might have improved the signal quality by minimizing any potential chromatin structure changes during the nucleosome isolation procedure, leading to the identification of nucleosome positions at a higher confidence level. We tested this hypothesis by isolating gel-extracted, ~150-bp fragments from partially digested (at two different digestion levels) cross-linked A375 chromatin and comparing those results to our original data (uncross-linked nucleosomal DNA, **Supplementary Discussion**). Whereas ~65% of previously identified nucleosomes could be reproduced with cross-linking of cells, the signal-to-noise ratio dropped and the data contained many small wavy peaks (<100 bps) that were not observed with noncross-linked samples. It is possible that cross-linking increases the level of association of nonhistone proteins with DNA, resulting in additional MNase-resistant nonnucleosomal fragments. Therefore, we do not consider partial digestion of cross-linked chromatin as an advantageous method for global nucleosome analysis in human cells.

The microarray approach successfully detected the positioned nucleosomes previously reported in eight human promoters (**Supplementary Notes** online and **Fig. 1b**). Additionally, as independent biochemical validation, we performed ChIPs at nucleosome resolution using anti-histone H3 antibody and conducted PCR (qPCR) reactions on different regions of the *BRCA1*, *CCN1*, *UGDH* and *CBLL1* promoters. In all cases, histone-associated DNA exhibited quantitatively distinct peaks compared to the neighboring troughs, and paralleled the patterns observed using the nucleosome tiling array method (**Fig. 1c,d** and **Supplementary Data** online). We also searched for short sequences differentially enriched in peaks relative to troughs. We found TATAAA, TATATA, GCGCGC and AAAAAA to be enriched in troughs, and TTCGA and CTGCTG to be enriched in peaks, all with profound statistical significance (**Supplementary Data**) and in agreement with previous publications[12–14]. Although micrococcal nuclease displays detectable sequence specificity toward naked DNA under some conditions[15], its preferred recognition sequences were notably underrepresented in the trough regions identified by our assay (**Supplementary Discussion**).

Nucleosomes are important regulators of transcription because they limit DNA accessibility[16]. Recent ChIP-chip studies in yeast[17,18] and fruit flies[19] suggest that the promoters of active genes are depleted of histones. At higher resolution, there is a nucleosome-free region flanked on both sides by positioned nucleosomes upstream of the start codon in yeast[7]. To examine whether a similar pattern exists in human cells, we compared nucleosome localization in expressed and unexpressed promoters within three cell lines (A375, IMR90, MALME) by cross-comparison to microarray expression profiling. We observed a sharp average signal drop at transcription start sites (TSS) of expressed genes, consistent with nucleosome depletion (**Fig. 2a** and **Supplementary Discussion**). Expressed genes were more likely ($P < 0.001$) to have a trough region spanning at least 100 bp at TSS compared to unexpressed genes, although troughs were occasionally seen among genes considered to be 'unexpressed'. It is possible that expression of these seemingly unexpressed genes having a trough at their TSS is underestimated by the expression microarray; or

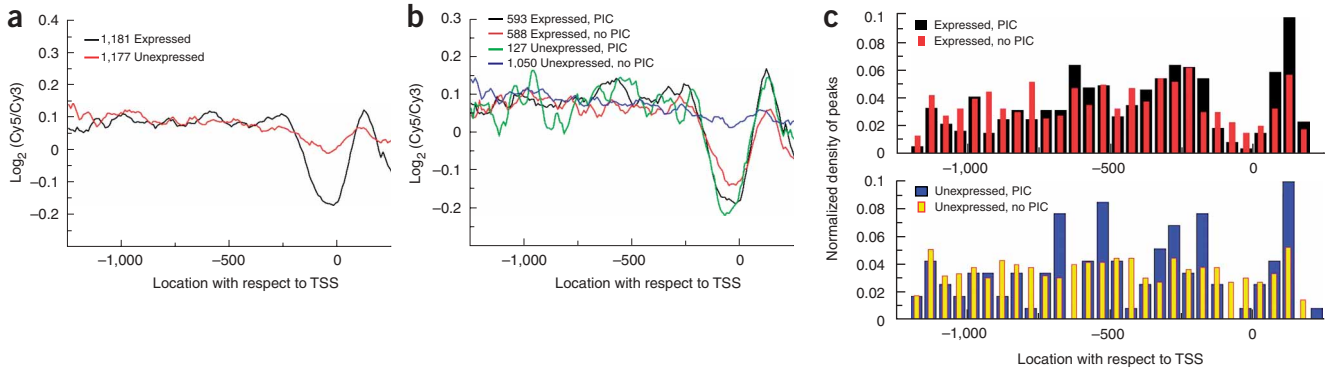

Figure 2 Nucleosome-free regions at transcription start sites of expressed genes or genes with preinitiation complexes (PIC) at their promoters. (**a**) Promoters were aligned at TSS and average probe signals were calculated. Expressed genes exhibited characteristic depletion of nucleosomes around the TSS in IMR90 and other cell lines (**Supplementary Discussion**). (**b**) IMR90 promoters were partitioned into four classes depending on the presence of a PIC and gene expression status[11]. Expressed genes or genes with a PIC in the promoter have a nucleosome-free region around TSS in IMR90, whereas unexpressed genes without PICs have a random distribution of positioned nucleosomes in their promoters. (**c**) The distribution of positioned nucleosomes in the four promoter classes in IMR90. *Y*-axis indicates the number of positioned nucleosomes found at a certain distance away from the TSS normalized by the total number of genes in each class. The distribution of positioned nucleosomes in unexpressed genes without a PIC (yellow bars) is uniform, whereas expressed genes or genes with a PIC tend to have fewer positioned nucleosomes around TSS and more surrounding the TSS.

alternatively chromatin structure at these promoters may have been modified so that these genes are poised for rapid expression under certain conditions[20]. To examine this latter possibility, we compared our data from IMR90 cells to the recent ChIP-chip analysis of transcription preinitiation complexes (PIC) in the same cell line[11]. In this study, human promoters were classified into four categories based upon gene expression status and the presence of PICs within promoter regions. We calculated the average signal and positioned nucleosome distribution along each promoter class. Three of the categories (expressed with or without PIC, and unexpressed with PIC) displayed positioned nucleosomes before and after the TSS, with the TSS being nucleosome depleted (**Fig. 2b**,**c**). The fourth category of genes (unexpressed without PIC) exhibited a relatively uniform distribution of positioned nucleosomes in the promoter regions analyzed without nucleosome depletion at the TSS. Most of the unexpressed genes with a trough at the TSS have a PIC located in the promoter, adding support to our hypothesis that these genes might indeed have a promoter chromatin structure that allows rapid transcription induction (or that they represent 'false negatives' in the expression profiling analyses). Furthermore, the average distance (~130 bp) between the two nucleosomes flanking the TSS in expressed genes or genes with PIC was too short to be occupied by another nucleosome, suggesting that the flanking positioned nucleosomes might function to limit nucleosome occupancy at the TSS.

Although nucleosomes are thought to limit accessibility to regulatory factors[1,2], no direct *in vivo* genome-scale test of this hypothesis has been provided in human cells. To this end, we carried out ChIP-chip analysis for the melanocyte transcription factor and melanoma oncogene *MITF*[21] in MALME and compared it to nucleosome positions within the same cells. We observed that 77% of microphthalmia-associated transcription factor (MITF)-occupied sites contain the consensus binding-site within linker regions surrounded by positioned nucleosomes ($P = 8 \times 10^{-5}$, **Fig. 3**, **Supplementary Data** and **Supplementary Discussion**), suggesting that MITF binds preferentially to nucleosome-free regions in human promoters. Therefore, this result corroborates studies showing that yeast transcription-factor binding sites are generally nucleosome free[7,22]. In addition, more highly conserved regions in the human genome tended to reside in nucleosome-free locations ($P = 3.6 \times 10^{-11}$, **Supplementary Discussion**), suggesting that most functionally important DNA sequences are indeed nucleosome free (**Fig. 3** and **Supplementary Data**). The binding of transcription factors and other regulatory machinery to nucleosome-depleted regions could explain why we observed nucleosome phasing (the distance between adjacent nucleosomes) to be variable in human promoters. In contrast, a more stereotypical pattern of positioned nucleosome spacing was observed surrounding the nucleosome-free regions in yeast promoters[7].

Although most identified positioned-nucleosomes were conserved across several cell lines (71% of positioned nucleosomes appeared in at least two cell lines, 51% in at least three cell lines), we observed many cases where the differences might indicate biological significance (**Supplementary Table 1** online). For instance, the *SILV* gene is active

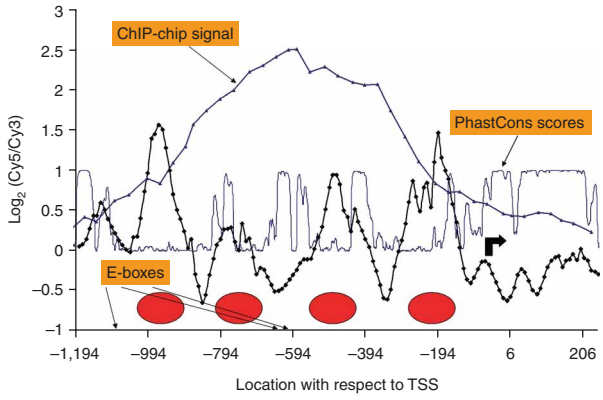

Figure 3 MITF binding sites are mostly nucleosome-free. The figure represents the MALME *GABARAP* promoter. Black line is the average of three MALME replicates; blue with dots, the ChIP-chip signal; and thin blue, the PhastCons conservation scores. *Y*-axis denotes the denoised ratios of Cy5 (nucleosomal DNA) and Cy3 (input DNA) intensities in $\log_2$ scale. The ChIP-chip signal covers a broad region including three E-boxes (CACGTG at –606, CATGTG at –633 and at –1,100). The maximum ChIP-chip signal comes from location –600 where two E-box elements (*MITF* consensus sites) are present within a trough.

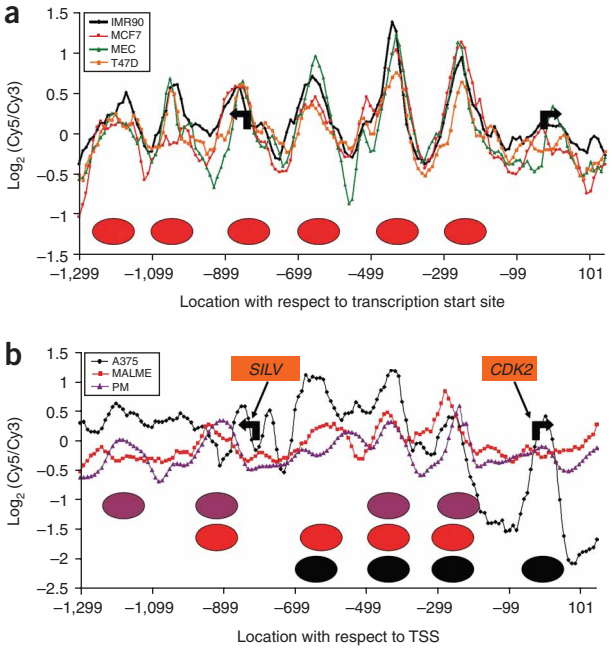

Figure 4 Variations in nucleosome positioning at the *CDK2-SILV* promoter locus correlate with lineage-specific *SILV* expression patterns, because the *SILV* gene is expressed selectively in melanocytes and melanomas[23]. (**a**) *CDK2-SILV* promoter in IMR90, MCF7, MEC and T47D. (**b**) *CDK2-SILV* promoter in A375, MALME and primary melanocytes (PM). In A375, there is a positioned nucleosome at the *CDK2*-annotated TSS even though CDK2 is expressed. This TSS might have been incorrectly annotated, because in all samples there is a low-signal region centered at –99, suggesting that the actual TSS may be located ~100 bp upstream of the annotated site. *Y*-axis denotes the denoised ratios of Cy5 (nucleosomal DNA) and Cy3 (input DNA) intensities in $\log_2$ scale.

in melanocytes and melanoma where MITF is expressed, but not in breast epithelial cells and breast cancer cells where MITF is absent or much less abundant[23]. In agreement with these observations, the TSS of *SILV* was nucleosome free in A375, MALME and primary melanocytes (**Fig. 4**), but occupied by a positioned nucleosome in nonmelanocytes (IMR90, MCF7, T47D and MEC). The positioned nucleosome at the *SILV* TSS and the surrounding compact nucleosome pattern may suppress *SILV* expression in the nonmelanocyte lines (or the absence of MITF may 'permit' nucleosome occupancy of the MITF binding site).

We have developed a framework that combines experimental and computational approaches to map chromatin structure at high resolution in human promoters. We found that functional *cis*-regulatory elements such as TSS and MITF binding sites tend to be nucleosome free. The described microarray platform and data analysis tool for rapid and robust determination of positioned nucleosomes in human cells might enable analysis of the interface between chromatin and gene expression in human development and disease.

METHODS

Mononucleosomal and input DNA preparation. T47D, MCF7, A375, MALME and IMR90 cells were grown and maintained according to the directions from American Type Culture Collection. MECs were commercially obtained from Cambrex and cultured according to their instructions. Primary melanocytes were isolated and maintained as described[24]. We used an optimized micrococcal nuclease (MNase) digestion protocol[25]. The cells (grown to 60–70% confluence) were trypsinized and washed once with Solution A (300 mM sucrose, 60 mM KCl, 35 mM HEPES pH 7.4, 5 mM K_2HPO_4, 5 mM $MgCl_2$, 0.5 mM $CaCl_2$) quickly and gently. The cells were then resuspended in Solution B (300 mM sucrose, 60 mM KCl, 15 mM NaCl, 35 mM HEPES pH 7.4, 5 mM K_2HPO_4, 5 mM $MgCl_2$, 3 mM $CaCl_2$) in 1.5 ml volume. NP-40 was added to 0.05% and mixed by pipetting. We added 25 U or 200 U of MNase (Worthington Biochemicals) to each reaction and incubated at 25 °C for 5 min. The reaction was stopped by adding 0.5 ml Solution C (100 mM EDTA, 4% SDS). The samples were then treated with RNAse A (0.1 mg/ml) for 1 h at 37 °C and proteinase K (0.1 mg/ml) overnight at 50 °C. DNA was purified by phenol/chloroform extractions and ethanol precipitation. The isolated DNA was run on a 1.5% agarose gel, and the band corresponding to mononucleosomes was gel-extracted usingQiaQuick Gel Extraction Kit (Qiagen). On average, low-level digestion (25 U MNase) led to a recovery of 0.015% of the entire DNA as mononucleosomal, whereas this number was 0.09% for high-level (200 U MN) digestion. We combined equal quantities of mononucleosomal DNA from low- and high-level digestions to have an equal representation of genomic regions that have variable sensitivity to MNase.

To prepare the input DNA, we isolated genomic DNA using the DNeasy Tissue Kit (Qiagen) and digested it with hydroxyl radical–based cleavage in a sequence-independent manner as described[26]. Reaction conditions were adjusted to have a final DNA size distribution of 100–200 bps. The reactions were cleaned with QiaQuick Gel Extraction Kit.

Custom tiling array design and hybridizations. The custom tiling array (NimbleGen Systems) covered the promoters of 1,346 genes in the Affymetrix Human Cancer G110 Array and 2,346 randomly selected RefSeq genes. The 1.5-kb repeat-masked region of each promoter (from –1,250 to +250) was tiled with 50-mer probes that overlapped by 10 bps. We eliminated potentially cross-hybridizing probes by checking the uniqueness of each probe in the human genome. Microarray fabrication, sample labeling, hybridization and microarray scanning were performed by NimbleGen Systems as described[11]. In all cases, experimental samples (nucleosomal DNA) were labeled with Cy5 and input DNAs were labeled with Cy3. No efforts were undertaken to examine possible variability of nucleosome positioning in genomic regions with potential copy number changes.

Histone ChIP-Chip and qPCR. To validate the identified peak and trough regions, we conducted chromatin immunoprecipitations at nucleosome resolution by replacing the sonication step with MNase digestion[27]. H3 ChIPs (using Abcam ab1791 antibody) yielded consistently higher DNA amounts (60–70 ng DNA) after ChIPs compared to negative control pulldowns in the absence of antibodies and in the presence of anti-HA antibody (4–5 ng Abcam ab9110). Immunoprecipitated DNA was quantified using the Picogreen dsDNA Quantitation Kit (Invitrogen).

The real-time PCR primers (**Supplementary Data**) were designed to amplify either the regions identified as peaks or linker regions. The amplicon sizes were kept between 60–110 bps to maintain sufficient nucleosome and linker DNA resolution. Quantitative real-time PCR was performed with 1 ng ChIPed DNA and 10 ng of total genomic DNA using iCycler and SYBR green iQ reagent (Bio-Rad). The threshold cycle values, calculated automatically by theiCycle iQ Real-Time Detection System Software (Bio-Rad), were used to estimate the fold enrichment of the tested peak or trough region in immunoprecipitated DNA over the unenriched genomic DNA, as described[11].

Gene expression analysis. RNA from A375 was extracted in biological duplicates with Trizol reagent (Invitrogen) and further purified using RNeasy Mini Kit (Qiagen) according to the manufacturer's recommendations. The purified total RNAs were hybridized to Affymetrix HG-U133Av2.0 arrays. The resulting hybridization data were analyzed using MAS 5.0 to determine the detection calls as present (P), marginal (M) or absent (A). The IMR90 and MALME expression profiles were obtained from refs. 11 and 21, respectively. The Affymetrix probes were remapped to the newest annotated RefSeq genes[28] and the precise numbers of expressed and unexpressed genes are provided in **Supplementary Data**. The binding sites of PIC in IMR90 were also mapped to the promoters on our tiling array; and in IMR90, 610 of the 1,181 expressed genes and 159 of the 1,177 unexpressed genes had PIC binding sites in the promoter regions tiled on our array.

MITF ChIP-Chip experimental design and analysis. Chromatin immunoprecipitation for MITF in MALME was performed following a published protocol[23]. We amplified 1 ng ChIPed sample and 1 ng unenriched ChIP input DNA side by side using ligation-mediated PCR[11]. Amplified DNAs were biotin-labeled[10] and hybridized to Affymetrix Promoter Tiling Arrays. We hybridized three experimental and two input replicates, and the resulting data were analyzed using MAT[29]. At the cutoff of $P = 1 \times 10^{-5}$, MAT predicted 117 MITF binding sites in the regions tiled on our custom array.

Nucleosome data processing and statistical analysis. The nucleosome datasets were first processed with wavelet denoising, a nonparametric regression analysis for removing high-frequency local noise. The denoised data from different cell lines and replicates were then quantile normalized (**Supplementary Methods**). Nucleosome positions were identified by applying a robust edge-detection algorithm called Laplacian of Gaussian (**Supplementary Methods**), which is a generalized second-derivative test searching for inflection points.

Accession numbers. The microarray data are available from Gene Expression Omnibus under accession number GSE6385.

Note: Supplementary information is available on the Nature Biotechnology website.

ACKNOWLEDGMENTS

We thank H. Widlund, E. Feige, V. Igras, I. Davis, W. Li and C. Meyer for helpful discussions and support. This work was supported by a grant from the US National Institutes of Health to D.E.F. and the Claudia Adams Barr Award for Innovative Basic Cancer Research to X.S.L. D.E.F. is Distinguished Clinical Scholar of the Doris Duke Charitable Foundation, and Charles and Jan Nirenberg Fellow in Pediatric Oncology at Dana-Farber Cancer Institute. J.S.S. was supported by the Claudia Adams Barr Award from Dana Farber Cancer Institute.

COMPETING INTERESTS STATEMENT

The authors declare that they have no competing financial interests.

Published online at http://www.nature.com/naturebiotechnology/
Reprints and permissions information is available online at http://npg.nature.com/reprintsandpermissions

1. Lu, Q., Wallrath, L.L. & Elgin, S.C. Nucleosome positioning and gene regulation. *J. Cell. Biochem.* **55**, 83–92 (1994).
2. Widom, J. Structure, dynamics, and function of chromatin *in vitro*. *Annu. Rev. Biophys. Biomol. Struct.* **27**, 285–327 (1998).
3. Lee, T.I. & Young, R.A. Transcription of eukaryotic protein-coding genes. *Annu. Rev. Genet.* **34**, 77–137 (2000).
4. Workman, J.L. & Kingston, R.E. Alteration of nucleosome structure as a mechanism of transcriptional regulation. *Annu. Rev. Biochem.* **67**, 545–579 (1998).
5. Becker, P.B. & Horz, W. ATP-dependent nucleosome remodeling. *Annu. Rev. Biochem.* **71**, 247–273 (2002).
6. Mellor, J. The dynamics of chromatin remodeling at promoters. *Mol. Cell* **19**, 147–157 (2005).
7. Yuan, G.C. *et al.* Genome-scale identification of nucleosome positions in *S. cerevisiae*. *Science* **309**, 626–630 (2005).
8. Segal, E. *et al.* A genomic code for nucleosome positioning. *Nature* **442**, 772–778 (2006).
9. Ioshikhes, I.P., Albert, I., Zanton, S.J. & Pugh, B.F. Nucleosome positions predicted through comparative genomics. *Nat. Genet.* **38**, 1210–1215 (2006).
10. Carroll, J.S. *et al.* Chromosome-wide mapping of estrogen receptor binding reveals long-range regulation requiring the forkhead protein FoxA1. *Cell* **122**, 33–43 (2005).
11. Kim, T.H. *et al.* A high-resolution map of active promoters in the human genome. *Nature* **436**, 876–880 (2005).
12. Mucha, M., Lisowska, K., Goc, A. & Filipski, J. Nuclease-hypersensitive chromatin formed by a CpG island in human DNA cloned as an artificial chromosome in yeast. *J. Biol. Chem.* **275**, 1275–1278 (2000).
13. Reid, D.G., Salisbury, S.A., Brown, T. & Williams, D.H. Conformations of two duplex forms of d(TCGA) in slow-exchange equilibrium characterized by NMR. *Biochemistry* **24**, 4325–4332 (1985).
14. Wang, Y.H., Amirhaeri, S., Kang, S., Wells, R.D. & Griffith, J.D. Preferential nucleosome assembly at DNA triplet repeats from the myotonic dystrophy gene. *Science* **265**, 669–671 (1994).
15. Horz, W. & Altenburger, W. Sequence specific cleavage of DNA by micrococcal nuclease. *Nucleic Acids Res.* **9**, 2643–2658 (1981).
16. Anderson, J.D. & Widom, J. Sequence and position-dependence of the equilibrium accessibility of nucleosomal DNA target sites. *J. Mol. Biol.* **296**, 979–987 (2000).
17. Lee, C.K., Shibata, Y., Rao, B., Strahl, B.D. & Lieb, J.D. Evidence for nucleosome depletion at active regulatory regions genome-wide. *Nat. Genet.* **36**, 900–905 (2004).
18. Pokholok, D.K. *et al.* Genome-wide map of nucleosome acetylation and methylation in yeast. *Cell* **122**, 517–527 (2005).
19. Mito, Y., Henikoff, J.G. & Henikoff, S. Genome-scale profiling of histone H3.3 replacement patterns. *Nat. Genet.* **37**, 1090–1097 (2005).
20. Hoffmann, A., Oelgeschlager, T. & Roeder, R.G. Considerations of transcriptional control mechanisms: do TFIID-core promoter complexes recapitulate nucleosome-like functions? *Proc. Natl. Acad. Sci. USA* **94**, 8928–8935 (1997).
21. Garraway, L.A. *et al.* Integrative genomic analyses identify MITF as a lineage survival oncogene amplified in malignant melanoma. *Nature* **436**, 117–122 (2005).
22. Bernstein, B.E., Liu, C.L., Humphrey, E.L., Perlstein, E.O. & Schreiber, S.L. Global nucleosome occupancy in yeast. *Genome Biol.* **5**, R62 (2004).
23. Du, J. *et al.* Critical role of CDK2 for melanoma growth linked to its melanocyte-specific transcriptional regulation by MITF. *Cancer Cell* **6**, 565–576 (2004).
24. McGill, G.G. *et al.* Bcl2 regulation by the melanocyte master regulator Mitf modulates lineage survival and melanoma cell viability. *Cell* **109**, 707–718 (2002).
25. Chen, C. & Yang, T.P. Nucleosomes are translationally positioned on the active allele and rotationally positioned on the inactive allele of the HPRT promoter. *Mol. Cell. Biol.* **21**, 7682–7695 (2001).
26. Zhang, Y. *et al.* Reproducible and inexpensive probe preparation for oligonucleotide arrays. *Nucleic Acids Res.* **29**, E66 (2001).
27. Kouskouti, A. & Talianidis, I. Histone modifications defining active genes persist after transcriptional and mitotic inactivation. *EMBO J.* **24**, 347–357 (2005).
28. Dai, M. *et al.* Evolving gene/transcript definitions significantly alter the interpretation of GeneChip data. *Nucleic Acids Res.* **33**, e175 (2005).
29. Johnson, W.E. *et al.* Model-based analysis of tiling-arrays for ChIP-chip. *Proc. Natl. Acad. Sci. USA* **103**, 12457–12462 (2006).
30. Fivaz, J., Bassi, M.C., Price, M., Pinaud, S. & Mirkovitch, J. Precisely positioned nucleosomes are not essential for c-fos gene regulation *in vivo*. *Gene* **255**, 169–184 (2000).